Current Applied Physics 13 (2013) 890–893

Contents lists available at SciVerse ScienceDirect

Current Applied Physics

journal homepage: www.elsevier.com/locate/cap

Effect of current-induced magnetic field on magnetization dynamics in spin-torque nano-oscillator with point-contact geometry

Woo-Yeong Kim [a], Kyung-Jin Lee [a,b,*]

[a] Department of Materials Science and Engineering, Korea University, Seoul 136-701, Republic of Korea
[b] KU-KIST Graduate School of Converging Science and Technology, Seoul 136-713, Korea

ARTICLE INFO

Article history:
Received 17 October 2012
Accepted 13 January 2013
Available online 4 February 2013

Keywords:
Spin-torque nano-oscillator
Spin-transfer torque
Micromagnetics

ABSTRACT

We show micromagnetic simulation results for spin-torque nano-oscillator (STNO) with point-contact geometry. Numerical results obtained from three different models are compared in order to investigate the effect of current-induced Oersted field and non-uniform current distribution on the characteristics of STNO. It is found that the Oersted field and non-uniform current distribution affect the frequency and precession mode both qualitatively and quantitatively. An anisotropic emission of spin-waves is observed only when considering the Oersted field properly. Our results suggest that a realistic consideration of the current distribution and consequent Oersted field distribution is of critical important to design STNOs and to understand the characteristics of STNOs.

1. Introduction

The spin-transfer torque, the transfer of spin-angular momentum from a spin-polarized current to a local magnetization, was theoretically predicted by Slonczewski and Berger in 1996 [1,2]. Since its prediction, the spin-transfer torque has been studied extensively both theoretically and experimentally [3–26]. The spin-torque nano-oscillator (STNO) using the phenomenon that the spin-transfer torque excites a steady-state precession mode of magnetization in a thin ferromagnetic layer is of considerable interest because of its potential for high frequency devices [10,11,13–17,27–29]. Rippard et al. [11] reported experimentally that a single STNO with point-contact geometry allows a tunable frequency and a high quality factor. Especially, point-contact geometry has advantages for device performances such as a narrower linewidth than nano-pillar geometry and a possibility to enhance microwave power by utilizing phase-locking among multiple point contacts [13,14].

The current injection through magnetic nanostructures generates not only a spin-transfer torque, but also a current-induced Oersted field. Micromagnetic simulations [30,31] and X-ray imaging [32] have revealed that the Oersted field has an important role on current-induced magnetization dynamics in fully-patterned nanopillars. In nanopillar structures, the current-flow is confined in the patterned nanopillar region so that non-negligible current-induced Oersted field can form when a high density of current is injected. On the other hand, a point-contact geometry has a semi-infinite thin film below a contact. An electrical current passing through a point-contact spreads out into the whole film plane [33]. In this case, the Oersted field is not strong as in nanopillar structures, but its spatial distribution is non-uniform. Therefore, the distribution of current-flow and corresponding distribution of Oersted field have to be properly calculated to understand magnetization dynamics in STNOs with point-contact geometry.

Using micromagnetic simulation, we investigate the effect of the Oersted field on current-induced magnetization dynamics in a spin-valve structure with point-contact geometry. We find that the Oersted field affects the frequency spectrum and the coherency of magnetization dynamics both qualitatively and quantitatively, suggesting that the Oersted field induced by an electric current is important even in point-contact geometry.

2. Simulation models and methods

In this work, we performed numerical simulations by solving the Landau–Lifshitz–Gilbert equation with an additional spin torque term [1];

$$\frac{d\mathbf{M}}{dt} = -\gamma\left(\mathbf{M}\times\mathbf{H}_{\text{eff}}\right) + \frac{\alpha}{M_S}\mathbf{M}\times\frac{d\mathbf{M}}{dt} + \frac{\gamma\hbar}{2e}\frac{g}{M_S^2 t_F}J\mathbf{M}\times(\mathbf{M}\times\mathbf{p}), \quad (1)$$

* Corresponding author. Department of Materials Science and Engineering, Korea University, Seoul 136-701, Republic of Korea.
E-mail address: kj_lee@korea.ac.kr (K.-J. Lee).

1567-1739/$ – see front matter © 2013 Elsevier B.V. All rights reserved.
http://dx.doi.org/10.1016/j.cap.2013.01.028

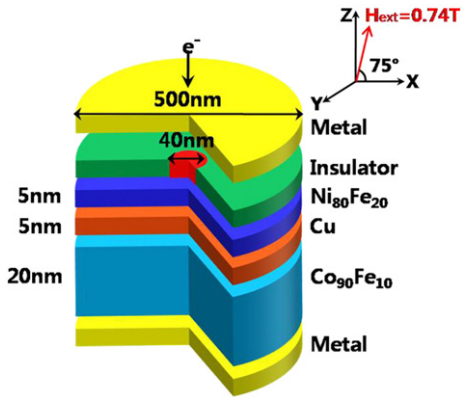

Fig. 1. A schematic diagram of the model system with point-contact geometry.

where γ ($=1.76 \times 10^7$ s^{-1} Oe^{-1}) is the gyromagnetic ratio, **M** is the magnetization vector of the free layer, $\mathbf{H}_{\text{eff}}$ is the effective magnetic field acting on the free layer, including the external field, the magnetostatic field, the exchange field, and the current-induced Oersted field, α ($=0.02$) is the Gilbert damping constant, **p** is the unit vector along the spin polarization direction, and M_S is the saturation magnetization of the free layer, g ($=0.4$) is the spin-torque efficiency factor, J is the current density, and t_F is the film thickness of the free layer.

As shown in Fig. 1, we use the 500×500 nm^2 mesa layer structures, consisting of 5 nm of Permalloy ($Ni_{80}Fe_{20}$) as a free layer, 5 nm of Cu as a spacer, and 20 nm of $Co_{90}Fe_{10}$ as a pinned layer. In our study, the magnetizations of pinned layer are fixed along to the external field direction and the magnetization dynamics at free layer is calculated to reduce calculation time. The size of a unit cell is $5 \times 5 \times 5$ nm^3 and the diameter of a point-contact is 40 nm. We apply an external magnetic external field (H_{ext}) of 0.74 T oriented 75° from the film plane to mimic experimental study performed by Kaka et al. [15]. The saturation magnetization of the free layer is 800 emu/cm^3 and that of the pinned layer is 1400 emu/cm^3. The electric current (I_e) injected through the point-contact is varied from 4 mA to 40 mA. Absorbing boundary condition is considered in order to prevent the reflection of spin-waves at the end of the simulation boundary, because the real device has an extended layer and its area is much larger than the modeling area [34–36]. We consider two cases of the current distribution; i.e. uniform current distribution (Fig. 2(a)) and realistic non-uniform current distribution (Fig. 2(b)). The non-uniform current distribution is obtained by solving the Laplace's equation. The electrical conductivities of $Ni_{80}Fe_{20}$, Cu, and $Co_{90}Fe_{10}$ are $4 \times 10^6\ \Omega^{-1}\ m^{-1}$, $2 \times 10^7\ \Omega^{-1}\ m^{-1}$, and $5 \times 10^6\ \Omega^{-1}\ m^{-1}$, respectively.

To study the role of current-induced Oersted field $\mathbf{H}_{\text{Oe}}$, simulation results obtained from three different models (model A, B, and C) are compared. In model A, $\mathbf{H}_{\text{Oe}}$ is not considered and the current distribution is assumed to be uniform and confined only in the contact area. In model B, $\mathbf{H}_{\text{Oe}}$ is considered with uniform current distribution. In model C, $\mathbf{H}_{\text{Oe}}$ is considered with a realistic non-uniform current distribution into the film plane.

3. Micromagnetic simulations: results and discussion

Here we focus mostly on the precession frequency of magnetizations in point-contact area and critical currents for different precession modes. The precession frequencies and critical currents obtained from the three models are summarized in Fig. 3(a) and (b), respectively. In the model A, the current for the onset of magnetization precession (I_{C1}) is 8.5 mA. For I_e smaller than 12 mA (I_{C2}), the free-layer magnetizations in the contact area show the pseudo-in-plane (pseudo-IP) precessional motion oriented to $\mathbf{H}_{\text{eff}}$ direction. In these current ranges, the precession angle increases with increasing I_e and thus the frequency decreases with increasing I_e, i.e. red shift (in the web version). When I_e is about 12 mA (I_{C2}), the phase transition of the precession mode occurs, i.e. transition from pseudo-IP to the out-of-plane (OOP) precession mode. The frequency increases with the current (blue shift in the web version) for 12 mA (I_{C2}) $\leq I_e <$ 22 mA (I_{C3}). In these current ranges, the free-layer magnetizations in point-contact area precess uniformly as like a single spin. For a higher current ($I_e >$ 22 mA (I_{C3})), the frequency decreases with I_e since the precession motion becomes complicated.

When we take into account $\mathbf{H}_{\text{Oe}}$ (model B and C), the frequency and precession mode of STNO become different both quantitatively and qualitatively in comparison with the results obtained from the model A. Since an electrical current induces a circular magnetic field around the current-flow line, it breaks the symmetry of the entire magnetic field distribution. In the model B, the onset current (I_{C1}) is about 8.5 mA, similar to that of the model A, but the precession frequency enhances compared to the model A (Fig. 3(a)). The frequency increases with I_e (blue shift), followed by a very narrow red shift region. The precession mode corresponding to the red shift is the pseudo-IP mode as in the model A, whereas the mode corresponding to the blue shift is not the OOP mode. At $I_e \geq$ 10 mA (I_{C4}), a vortex structure is developed, resulting in an anisotropic spin-wave generation. We will discuss this

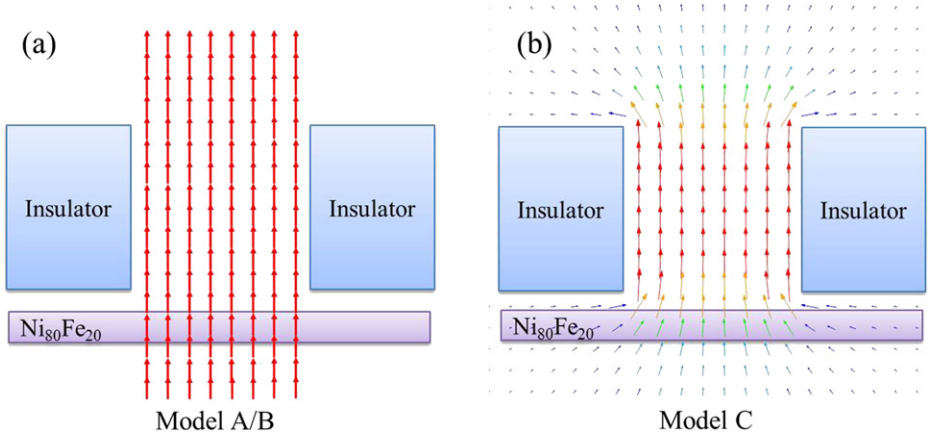

Fig. 2. The current distribution (arrows in the figure) of three different models; (a) model A and B, and (b) model C.